

# High Efficient Photovoltaics in Estonia

M. Altosaar, S. Bereznev, M. Kauk, M. Krunks, J. Krustok, E. Mellikov,  
J. Raudoja, T. Varema

Tallinn Technical University, Estonia

The aim of this paper is to summarize results of recent research at Tallinn Technical University on different materials and technologies for PV solar cells and technological developments in the field of polycrystalline PV solar cells. The following topics are addressed in this paper:

1. Photoluminescence of different ternary compounds;
2. Thin films and thin film structures by different chemical methods;
3. Photovoltaic structures based on electrically conductive polymers and CIS;
4.  $\text{CuInSe}_2$  monograin powders with tailored composition and structure;
5. Technological developments and photoelectrical parameters of monograin layer solar cells.

## 1. Photoluminescence studies.

Photoluminescence (PL) is a widely used method to study the defect structure in semiconductor materials. A large number of studies have been published also for the chalcopyrite compound  $\text{CuInSe}_2$  (CIS). PL spectra of CIS crystals and thin films are very sensitive to the deviation from the ideal stoichiometry and also to the doping. We have studied the role of Na and K in CIS single crystals [1]. We proposed a model that the so-called B- band at 0.991 eV is caused by a solid solution phase of CIS with Na or K, see Figure 1. The measured spectrum shows two bands at 0.991 eV (B-band) and 0.973 eV (A-band)[1].

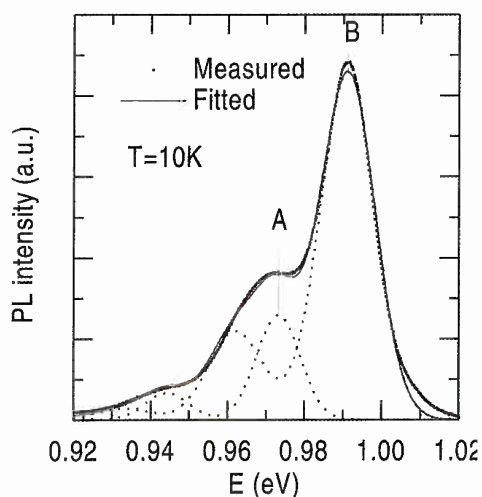


Figure 1: Typical photoluminescence spectrum of a stoichiometric  $\text{CuInSe}_2$  crystal [1]

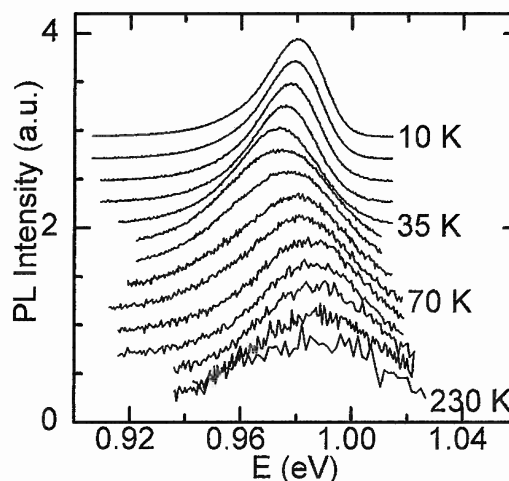
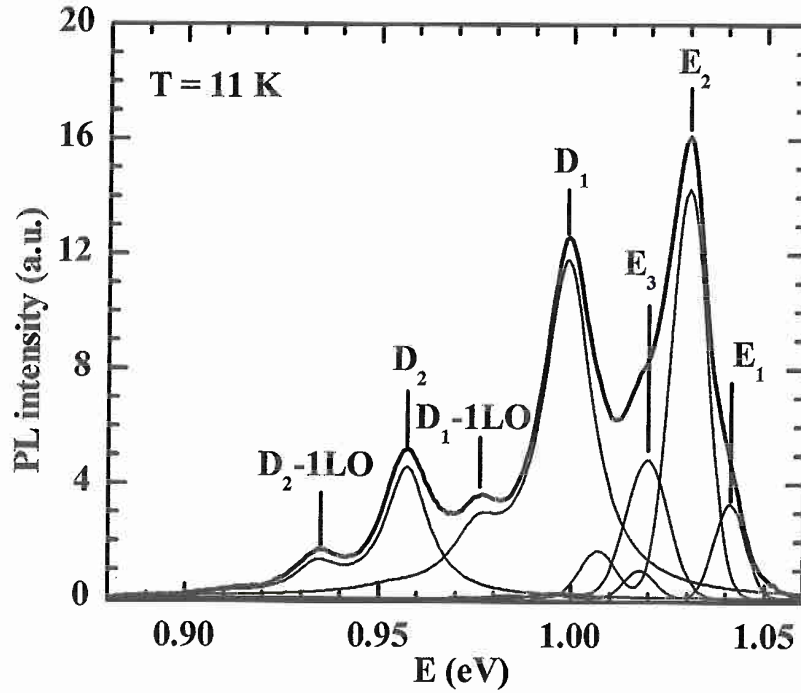


Figure 2: Normalised PL spectra of  $\text{CuInTe}_2$  measured at different temperatures. [2]

Lot of research has been done lately also with chalcopyrite tellurides: CuInTe<sub>2</sub>, AgInTe<sub>2</sub> and others. Chalcopyrite tellurides are less studied than selenides and sulphides and therefore it is important to gain information about defect states also from these materials in order to use these materials in solar cell structures. For example, In-rich CuInTe<sub>2</sub> shows a very similar PL spectra to CIS [2] see Figure 2. At the same time the nearly stoichiometric CuInTe<sub>2</sub> shows lot of defects related PL bands, see Figure 3 [3].



**Figure 3:** PL spectra of CuInTe<sub>2</sub> single crystal at 11 K. Measured PL spectra were fitted using five different peaks and their phonon replicas [3].

The proposed defects and their possible chemical origin are given in Table 1:

**Table 1:** Experimental values of PL band positions for CuInTe<sub>2</sub> compared with theoretical calculations. Activation energies were calculated with  $E_g = 1.06$  eV.

PL Band	$h\nu_{max}$ (eV)	$E_a$ (meV)		Possible origins [4]
		Experimental	Theoretical [4]	
E1	1.041			Excitons
E2	1.030	30	26	$V_{Te}^{\bullet}$ , $In_{Cu}^{\bullet}$
E3	1.019	41	37	$In_i^{\bullet}$
D1	0.999	61	70	$V_{Cu}'$ , $Te_{In}'$ , $Cu_{Te}'$
D2	0.957	103	120	$Te_i'$ , $Cu_{In}'$

Very interesting features of deep PL bands in CuInS<sub>2</sub> were also lately found [5].

## 2. Thin films and thin film structures by different chemical methods

The manufacturing of materials by chemical methods needs a good knowledge on the formation of materials and their properties to produce materials with controlled properties for high efficiency devices. Therefore, the fundamental research in the field of the chemical processes should be performed. The approach applied to the formation chemistry studies includes the study of processes in the spray solution followed by the thermoanalytical study of the complexes as a model compounds for spray. Our group firstly developed the approach for ZnO, CdS and  $\text{Cu}_x\text{S}$  formation in spray pyrolytic process [6-9]. During last years it was applied for ZnS and  $\text{CuInS}_2$  [10, 11].

It is shown that using appropriate metal chlorides and thiocarbamide (tu) as starting materials, there occurs complexation with formation of  $\text{Me}(\text{tu})_n\text{Cl}_m \cdot y\text{H}_2\text{O}$  ( $n = 1, 3; m = 1, 2; y = 0, 0.5, 1$ ) in aqueous solution.  $\text{Zn}(\text{tu})_2\text{Cl}_2$  is a precursor for ZnS and  $\text{CuInS}_2$  formation passes through the phases of  $\text{Cu}(\text{tu})\text{Cl} \cdot 1/2\text{H}_2\text{O}$  and  $(\text{NH}_4)_2\text{InCl}_5 \cdot \text{H}_2\text{O}$ , as established by chemical analysis, XRD and FTIR.

Thermal decomposition of precursors was studied up to  $1200^\circ\text{C}$  in dynamic inert ( $\text{N}_2$ ) and oxidative (air) atmospheres using simultaneous TG/DTA and TG/EGA techniques (Fig.1). XRD and IR were employed *ex situ* to resolve the reaction mechanism and products in each decomposition step. According to the thermoanalytical study it could be concluded that metal to ligand (tu) bonding in metal halogenide thiourea complexes is thermally stable up to  $200^\circ\text{C}$  and thermal decomposition of spray process precursors is a complicated multistep process where metal sulfide forms in the first decomposition stage at  $250^\circ\text{C}$ . At temperatures higher than  $250^\circ\text{C}$  the expelling of halogenide containing and organic residues occurs. The comparative study of CdS, ZnS and  $\text{Cu}_x\text{S}$  thin film formation is presented in [12]. In an inert atmosphere single phase metal sulphide films could be achieved at  $650 - 960^\circ\text{C}$  depend on the precursor. In air a compromise between the deposition temperature leading to oxidated phases and impurity level of metal sulfide films must sought after.

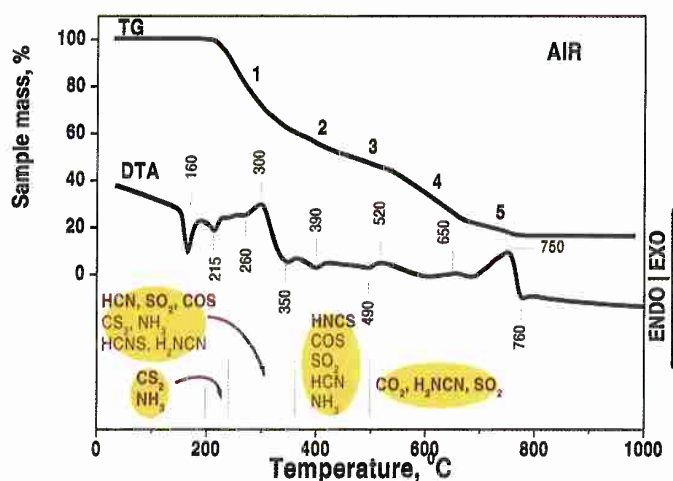


Figure 4: TG, DTA and DTG curves of  $\text{Zn}(\text{tu})_2\text{Cl}_2$  recorded in flowing air of  $80 \text{ ml min}^{-1}$  at the heating rate of  $10^\circ\text{C min}^{-1}$  on SeikoTG/DTA 320 instrument. The sample mass is 24.12 mg. Evolved gases in different decomposition steps as recorded by EGA-FTIR are shown [11]

CuInS<sub>2</sub> thin films were prepared by spray pyrolysis technique using CuCl<sub>2</sub>, InCl<sub>3</sub> and SC(NH<sub>2</sub>)<sub>2</sub> as starting chemicals. Aqueous solution of starting materials was deposited onto glass substrates (bare or with electrodes) using pneumatic spray system and nitrogen as a carrier gas. The structure, surface morphology and chemical composition of sprayed CuInS<sub>2</sub> films depending on the procedure parameters as growth temperature, Cu/In and S/Cu molar ratio in solution and following post-thermal treatments has been studied [13-15]. Structure and morphology of spray deposited CuInS<sub>2</sub> thin films was characterized by XRD and SEM, respectively, the composition of the films was studied by different chemical analysis techniques, EDS, RBS, FTIR [13, 14]. It is found that the growth temperature of 350-370 °C is the best settlement between the purity and oxidation. The crystallinity of sprayed films is determined by the Cu/In ratio in spray solution (Fig. 5). The films prepared from In-rich solutions are closely amorphous. The increase in the Cu/In in solutions significantly improves the crystallinity of the films and CuInS<sub>2</sub> films with chalcopyrite structure could be prepared from Cu-rich solutions. Crystallite size of 7, 44 and 120 nm was calculated for the films at Cu/In ratios in solution of 1.0, 1.1 and 2.0, respectively. The films prepared at Cu/In ≤ 1 have smooth surface whereas Cu-rich solutions lead to rough surface (Fig. 6). Cu<sub>x</sub>S phase segregating on the film surface is found to be responsible for the recrystallization process.

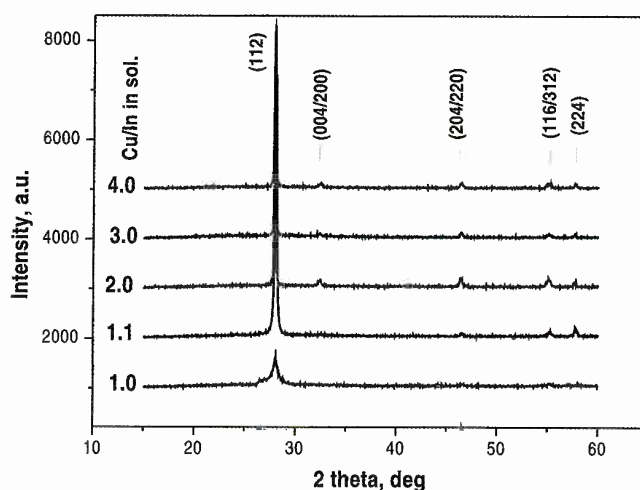


Figure 5: XRD patterns of KCN etched sprayed CuInS<sub>2</sub> films grown at T<sub>S</sub> = 360 °C using Cu/In molar ratio from 1.0 up to 4 in spray solution.

Chlorine, nitrogen and carbon containing residues are present in as-prepared CuInS<sub>2</sub> films as by-products of pyrolytical decomposition of intermediates. The growth temperature mainly controls the concentration of residues originated from precursors. The content of impurities in somewhat depends on the Cu/In in solution as the use of Cu-rich solutions results in lower impurity concentrations. Inversely to residues originated from the precursors, concentration of oxygen increases concurrently with the growth temperature.

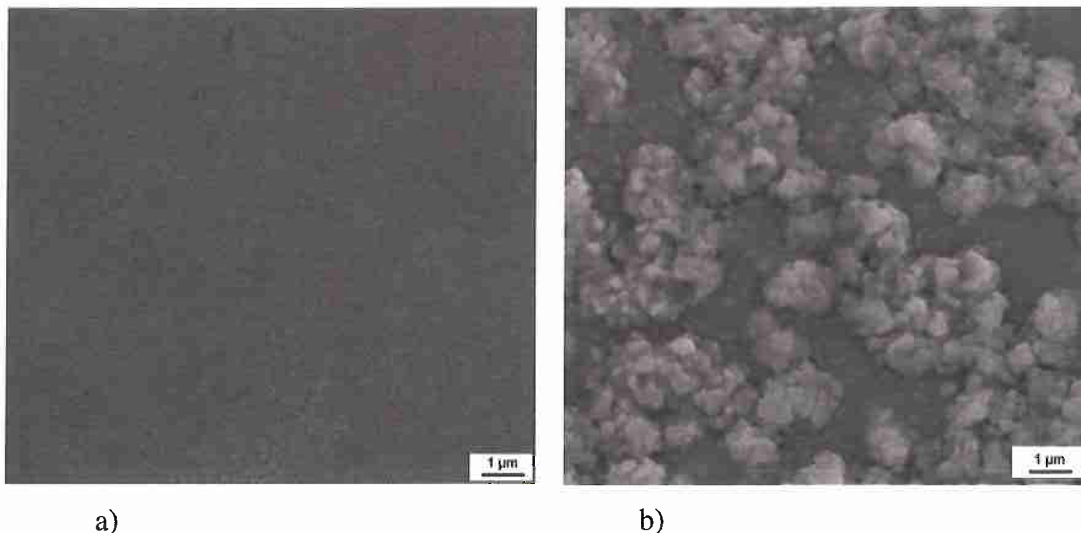


Figure 6: SEM micrographs of KCN etched spray deposited  $\text{CuInS}_2$  films prepared using the  $\text{Cu/In} = 1$  (a) and  $\text{Cu/In} = 2$  in spray solution.

Electrical resistivity of the films was characterized by four-point and conductivity type by hot probe methods, respectively [16]. Sprayed  $\text{CuInS}_2$  films show p-type conductivity and resistivity close to  $10 \Omega\text{cm}$  after thermal purification process. Carrier concentrations of  $10^{17} \text{cm}^{-3}$  were determined by C-V measurements on Schottky barriers  $\text{CuInS}_2/\text{Al}$  and p-n junctions in solar cells [17]. All layers sprayed  $\text{ZnO/CdS/CuInS}_2$  solar cells are reached the efficiency of 2.0 % what is the highest value reported for the cells by cost-effective spray method up to now (Fig. 7). The junction barrier height was determined by  $V_{\text{OC}}$  temperature dependent measurements (Fig. 8). Frequency swept admittance spectroscopy was applied to characterize the p-n junction characteristics [17]. It is found that interface recombination is the limiting factor of solar cell performance based on sprayed absorber.

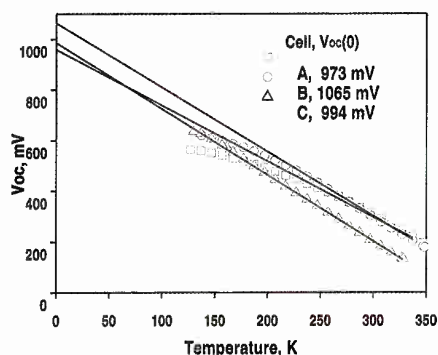


Figure 7: I-V curve of all layers sprayed  $\text{ZnO/CdS/CuInS}_2$  solar cell in dark and under AM1.5

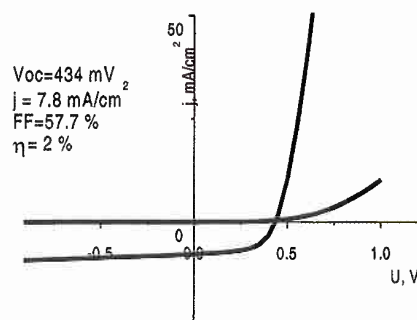


Figure 8:  $V_{\text{OC}}$  of sprayed  $\text{ZnO/CdS/CuInS}_2$  solar cell vs. temperature.  $\text{CuInS}_2$  prepared using  $\text{Cu/In} = 0.9$  (A), 1.0 (B), 1.1 (C) in spray solution [17].

The use of buffer layer is important in solar cells based on  $\text{TiO}_2$ . Indium (hydroxy) sulphide  $\text{In}_x(\text{OH})_y\text{S}_z$  (band gap 2.5 eV) as a buffer layer at the  $\text{TiO}_2$ /absorber interface effectively suppress the recombination. Photoelectrical measurements on solid-state cells with a stack of flat  $\text{TiO}_2$ , a wet-chemically applied  $\text{In}_x(\text{OH})_y\text{S}_z$  layer and a sprayed  $\text{CuInS}_2$  absorber layer on top of it reveal a characteristic diode curve with an energy conversion efficiency of 2.1 %, in contrast to the short circuiting observed for cells with  $\text{TiO}_2/\text{CuInS}_2$  alone [18].

### **3. Photovoltaic (PV) structures based on electrically conductive polymers and CIS**

Photovoltaic (PV) structures based on electrically conductive polymers (ECP) are currently intensively investigated in many laboratories with the aim to produce low-cost, large-area and flexible "plastic" photodiodes and solar cells [19, 20]. In the field of research of low-cost solar energy converters, hybrid organic-inorganic PV junctions in an all thin-film configuration deserve serious investigation [21, 22].

In present field our attention was focused on preparation and investigation of the hybrid ECP/copper-indium-chalcogenides PV structures, which result from ECP deposition on the CIS films. Combination of CIS with ECP, e.g. polyaniline (PANI), polypyrrole (PPy) and poly(3,4-ethylenedioxythiophene) (PEDOT) is attractive for use in thin-film PV cell structures. It should be noted, that PANI, PPy and PEDOT are well-known conductive polymers. The wide range of associated electrical, electrochemical and optical properties, coupled with good stability, makes these ECP potentially attractive for application as an active material of PV and others devices. These ECP always have p-type conductivity when doped with sulfonates, but the type of conductivity in CIS strongly depends on the composition and defects and may be p- or n-type. A number of PV structures on the basis of photoactive polycrystalline  $\text{CuInSe}_2$  (CISe) and  $\text{CuInS}_2$  (CIS) in combination with PANI, PPy and PEDOT were prepared using electrodeposition and casting techniques. The ECP layer is considered as an alternative to the inorganic p-type barrier layer on n-CISe or p-type buffer layer and window layer on CIS absorber layers in the cell structure.

Photoactive CISe thin films were deposited electrochemically on glass/ITO substrates from aqueous solutions containing  $\text{CuSO}_4$ ,  $\text{In}_2(\text{SO}_4)_3$  and  $\text{SeO}_2$ . As absorber layers, polycrystalline CIS thin films were synthesized on top of a layered structure on Cu tape substrate using a non-vacuum CISCuT technique [23]. All obtained polycrystalline films were annealed in vacuum for improving the crystalline structure and etched in 10% KCN to remove the additional phases.

In order to prepare the PV structures thin PPy films doped with  $\beta$ -naphthalene sodium sulfonate ( $\beta$ -NSA) were electrodeposited onto such prepared CIS films galvanostatically and potentiostatically in various conditions. It was found, that electrochemical polymerization of pyrrole to PPy on CIS surfaces is faster under white light irradiation, and the polymerisation starts at lower potential, than in the dark. Also, the PANI films doped with dodecylbenzene sulfonic acid (DBSA) were deposited onto n-CISe films from the chloroform solution of chemically synthesized soluble PANI using the drop-casting method. Thin PEDOT films doped with polystyrenesulfonate (PSS) were deposited onto the CIS films from an aqueous dispersion of PEDOT-PSS mixed with N-methylpyrrolidone, isopropanol, glycerin and epoxysilane additives using the spin-casting technique. In order to prepare stable PPy and PEDOT films of high quality with

a good adherence to the surface of inorganic semiconductors CISe and CIS, the optimal parameters of electrodeposition and spin-coating were selected experimentally.

All the investigated photovoltaic structures were fabricated as sandwich configurations glass/ITO/CISe/PANI/Ag, glass/ITO/CISe/PPy/Ag, Cu/CIS/PPy/i-ZnO/n-ZnO, Cu/CIS/PEDOT-PSS/i-ZnO/n-ZnO, Cu/CIS/PEDOT-PSS/Graphite dot, Cu/CIS/PEDOT-PSS/Au (semitransparent) and Cu/CIS/PEDOT-PSS/Au (grid) as shown in Figure 9.

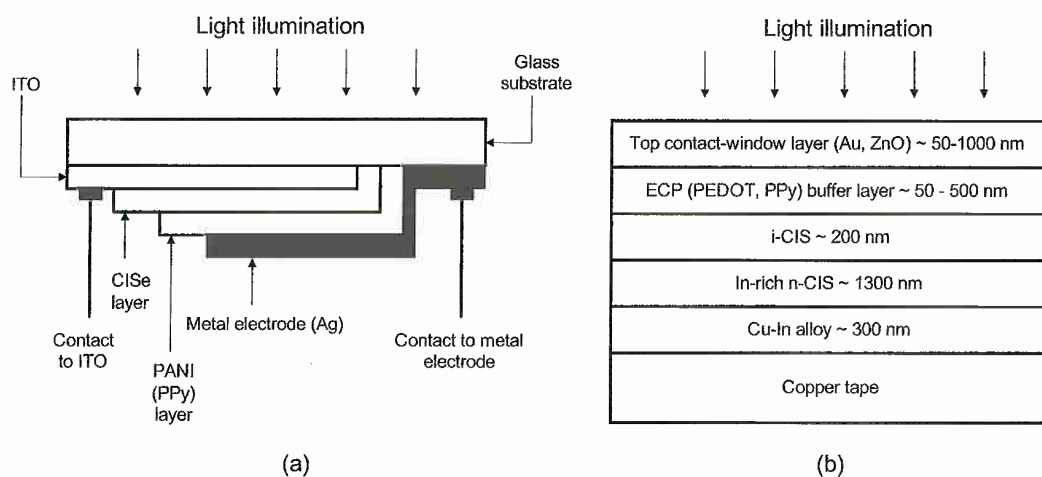


Figure 9: Schematic drawing of prepared PV structures: (a) – structures on glass/ITO substrates; (b) – structures on Cu-tape substrates

Table 2: Photovoltaic parameters of complete structures [24-30]

Structure	Open-circuit voltage $V_{oc}^*$ , [mV]	Short-circuit current density $I_{sc}^*$ , [mA/cm <sup>2</sup> ]	Fill-factor FF	Efficiency $\eta$ [%]
ITO/CISe(1-3-3)/PANI-DBSA/Ag	47	0.8	0.24	0.01
ITO/CISe(3-7-11)/PPy- $\beta$ -NSA /Ag	138	2.6	0.25	0.1
Cu/CIS/PPy- $\beta$ -NSA/i-ZnO/n-ZnO	509	6.5	0.47	1.5
Cu/CIS/PEDOT-PSS/Graphite dot	543	11.5	0.30	1.9
Cu/CIS/PEDOT-PSS/Au semitransparent	460	9.4	0.31	1.4
Cu/CIS/PEDOT-PSS/i-ZnO/n-ZnO	360	6.1	0.15	0.3
Cu/CIS/PEDOT-PSS/Au grid	510	20.2	0.40	4.1

\*Under white light illumination of 100 mW/cm<sup>2</sup>

Significant photovoltage and photocurrent of the fabricated PV structures have been observed under standard white light illumination with an intensity of 100 mW/cm<sup>2</sup>. All the measured PV parameters of investigated structures are presented in Table 2. The best structure Cu/CuInS<sub>2</sub>/PEDOT-PSS/Au grid showed an open-circuit voltage of 510 mV and a short-circuit current density of 20.2 mA/cm<sup>2</sup>. Hybrid PV structures on the

basis of  $\text{CuInSe}_2$ /ECP junctions described here have reached an efficiency less than 1%. Nevertheless the short circuit current is high and proves the value of the chosen approach.

#### 4. $\text{CuInSe}_2$ monograin powders with tailored composition and structure

The phase diagram of Cu-Se [31] shows that, at temperatures  $530^\circ\text{C}$  and higher, there should not exist any solid phase in the system used other than  $\text{CuInSe}_2$ . This gives a prerequisite to use melted binary Cu-Se phases for the synthesis and monograin growth process of  $\text{CuInSe}_2$  monograin powders [32-34]. In following other salts were used as fluxes in synthesis and monograin growth process. In case of binary Cu-Se phases the CuIn (1:1) alloy and CuSe were synthesized from their elements in evacuated quartz ampoules and were ground in an agate mortar before use in the powder growth process [32]. The growth temperature was varied in the range of 800-1025K. Crystals of the synthesised powder were of a uniform, round shape, with smooth surfaces (Fig 11). Temperature and duration of recrystallisation process could control Crystal size. Additionally crystal size could be tailored by chemical nature of flux used in growth process,

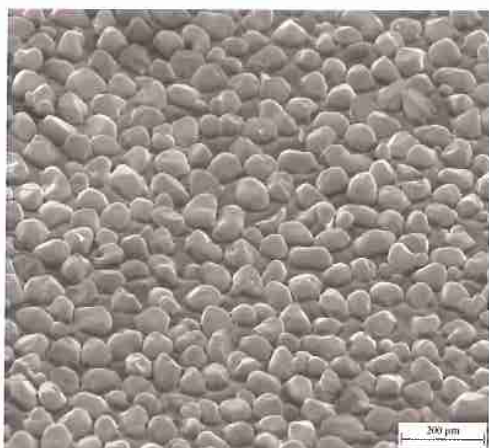


Fig 11. SEM picture of typical  $\text{CuInSe}_2$  monograin layer [35].

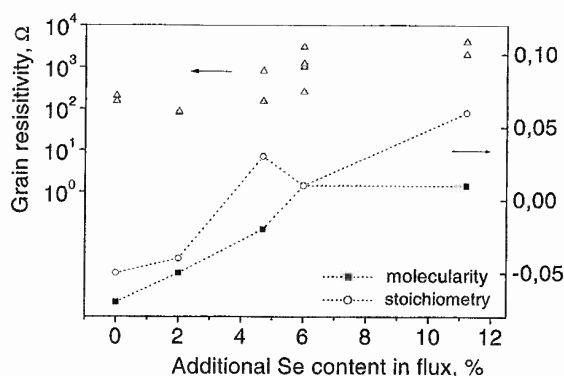


Fig.12. Influence of flux content on the chemical composition (molecularity and stoichiometry) and electrical resistivity of monograin  $\text{CuInSe}_2$  powders [35]

The composition of developed monograin powders could be tailored by composition and chemical nature of used flux and by additional thermal treatments in different atmospheres. The growth temperature did not notably influence the chemical composition of individual  $\text{CuInSe}_2$  crystals in the powders (determined by EDS). At the same time, the ratio (Cu/In) showed a tendency to increase whiles the Se content decreased (Fig. 12).

The electrical parameters and chemical composition of powder crystals could be tailored by treatments in different gas atmospheres.  $\text{CuInSe}_2$  powder materials were annealed in dynamic vacuum ( $10^{-2}$  torr) at different temperatures from 370K to 800K for a constant time period for the tailoring of the materials' electrical parameters. The results (Fig.13) reveal that the molecularity did not change in the annealing process up



to 725K for 15 minutes but the selenium already starts to be removed from materials at 370K. The grain resistivity increases up to 670K but at higher temperatures has a tendency to decrease.

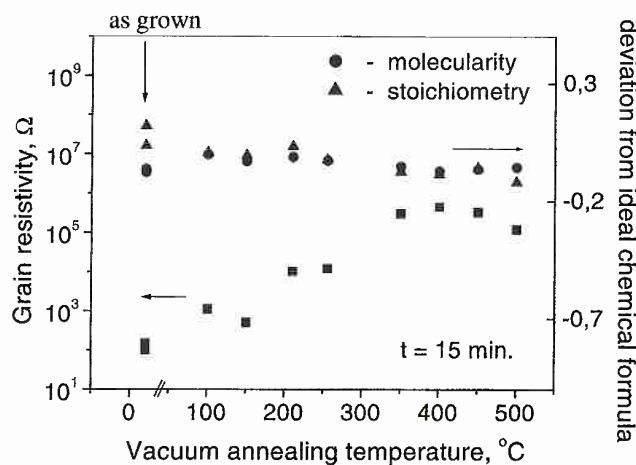


Fig. 13 Influence of vacuum annealing on the chemical composition of powders [35]

Treatment of powders under Se atmosphere has no remarkable effect on the volume composition of powder crystals. At the same time, the electrical conductivity of the powders changes by more than 3 orders of magnitude.

#### 4.1 Monograin solar cell technology and properties.

Monograin layer solar cell is represented on Figure 14.

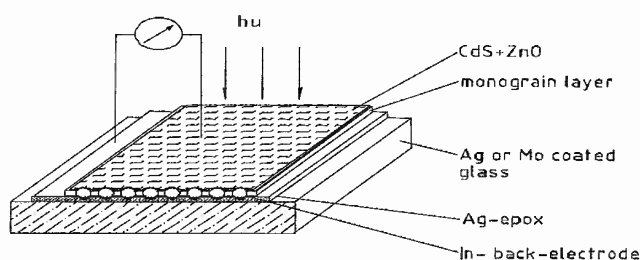


Figure 14: SC structure of monograin layer

At the moment our monograin layer solar cells show  $V_{oc}$  in the range of 500mV- a typical value for  $CuInSe_2$  material, see Figure 15. At the same time our MGL are characterised with the relatively low FF and quite high dark current values. All these facts indicate that the interface recombination is a prevailing loss mechanism although  $V_{oc}$  vs. T measurements show barrier high at the range of  $E_g$  of  $CuInSe_2$ , see Figure 16.

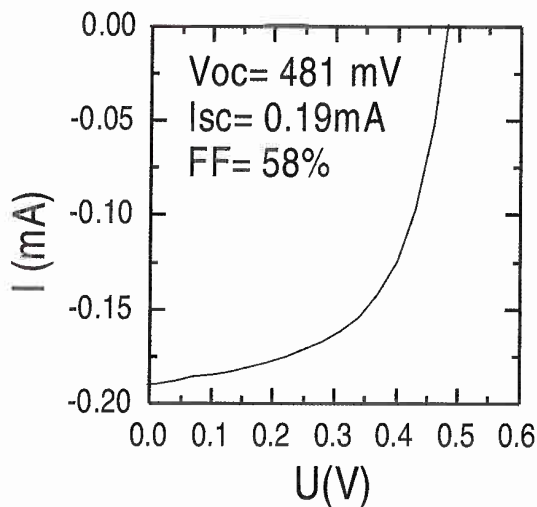


Figure 15: Typical I-V curve of r CIS monograin cell under standard  $100 \text{ mW/cm}^2$  illumination

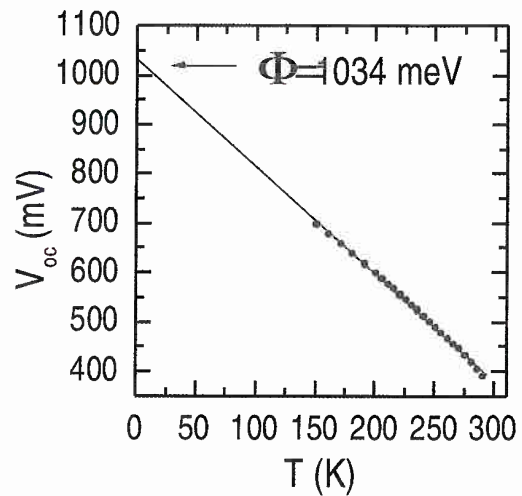


Figure 16:  $V_{oc}$  vs. T curve of MGL solar cell showing typical for  $\text{CuInSe}_2$  barrier height

## 5. Summary

On the base of our research we have shown that different chemical technique have perspective for producing cheap PV cell structures of different design. The studies to optimize the materials and used technologies will be continued in the future.

## 6. Acknowledgement

The financial support for this research in the field of solar energy materials and solar cells by EU FW5 projects NNE5-2002-00017, NNE5-2001-00544, NNE5-2002-00046, HRPN-CT-2000-00141 and by different Estonian Scientific Foundation grants is gratefully acknowledged.

## 7. References

- [1] J. Krustok, A. Jagomägi, J. Raudoja, and M. Altosaar, *Solar Energy Materials and Solar Cells* **79**, 401 (2003).
- [2] A. Jagomägi, J. Krustok, J. Raudoja, M. Grossberg, M. Danilson, and M. Yakushev, *Physica B* (in press)
- [3] A. Jagomägi, J. Krustok, J. Raudoja, M. Grossberg, and M. Danilson, *phys. stat. sol. (b)*, **237**, R3 (2003).
- [4] R. Márquez, C. Rincón, *Materials Letters* **40**, 66 (1999)
- [5] J. Krustok, J. Raudoja, and H. Collan, *Thin Solid Films* **387**, 195 (2001).
- [6] M. Krunk, O. Bijakina, T. Varema, V. Mikli, E. Mellikov, *Physica Scripta*, T79 (1999) 209-212

- [7] M. Krunk, J. Madarasz, L. Hiltunen, R. Mannonen, L. Niinistö, E. Mellikov, *Acta Chemica Scandinavica*, 51 (1997) 294-301.
- [8] M. Krunk, T. Leskelä, R. Mannonen, L. Niinistö, *J. Therm. Anal.*, 53 (1998) 355-364.
- [9] M. Krunk, T. Leskelä, I. Mutikainen, L. Niinistö, *J. Therm. Anal. and Cal.*, 56 (1999) 479-484.
- [10] M. Krunk, T. Leskelä, L. Niinistö, *Jap. J. Appl. Phys.*, 39, (2000) 181-186.
- [11] M. Krunk, J. Madarász, T. Leskelä, A. Mere, L. Niinistö, G. Pokol, *J. Therm. Anal. Cal.*, 72 (2003) 497-506.
- [12] M. Krunk, E. Mellikov, *Proceedings of SPIE*, vol. 4415, 2001, p.60-65.
- [13] M. Krunk, O. Bijakina, V. Mikli, H. Rebane, T. Varema, M. Altosaar, E. Mellikov, *Solar Cells and Solar Cell Materials*, 69, 1 (2001) 93-98.
- [14] M. Krunk, O. Kijatkina, H. Rebane, I. Oja, V. Mikli, A. Mere, *Thin Solid Films*, 403-404 (2002) 71-75.
- [15] O. Kijatkina, M. Krunk, A. Mere, B. Mahrov, L. Dloczik, *Thin Solid Films*, 431-432 (2003) 105-109.
- [16] M. Krunk, O. Kijatkina, J. Blums, I. Oja, A. Mere, E. Mellikov, *Proceedings 17-th European PVSEC, 22-26 Oct. 2001, Munich, Germany, published by WIP-Munich and ETA-Florence, 2002, v.2, p.1211-1214.*
- [17] A. Mere, O. Kijatkina, H. Rebane, J. Krustok, M. Krunk, *J. Phys. Chem. Solids*, 64 (2003) 2025-2029
- [18] J. Wienke, M. Krunk, F. Lenzmann, *Semiconductor Science and Technology* 18 (2003) 876-880.
- [19] C. J. Brabec, N. S. Sariciftci and J. C. Hummelen, *Advanced Functional Materials*, 2001, 11, No 1, 15-26.
- [20] L. Ding, M. Jonforsen, L. S. Roman, M. R. Andersson, O. Inganäs, *Synthetic Metals*, 2000, 110, № 2, 133-140.
- [21] P. Chartier, H. Nguyen Cong and C. Sene, *Solar Energy Materials and Solar Cells*, 1998, 52, 413-421.
- [22] P. J. Sebastian, S. A. Gamboa, M. E. Calixto, H. Nguyen-Cong, P. Chartier and R. Perez, *Semicond. Sci. Technol.*, 1998, 13, 1459-1462.
- [23] J. Penndorf, M. Winkler, O. Tober, D. Röser, K. Jacobs, *Solar Energy Mat. and Solar Cells*, 1998, 53, 285-298.
- [24] S. Bereznev, J. Kois, E. Mellikov, A. Öpik, *Proceedings of Baltic Polymer Symposium 2001, Tallinn, Estonia, October 11-12, 2001, p. 148-154.*
- [25] S. Bereznev, J. Kois, E. Mellikov, A. Öpik and D. Meissner, *Proceedings of Seventeenth European Photovoltaic Solar Energy Conference (München, Germany, October 22-26, 2001), 1 (2002), p. 160-163.*
- [26] S. Bereznev, I. Konovalov, J. Kois, E. Mellikov, A. Öpik, accepted of Organizing Committee of 21<sup>st</sup> Discussion Conference of P.M.M. / 9<sup>th</sup> International Conference ERPOS (14-18.07.2002, Prague). Accepted for publication in *Macromolecular Symposia*.

- [27] J. Kois, S. Bereznev, M. Altosaar, E. Mellikov, A. Öpik, accepted of Organizing Committee of 3<sup>rd</sup> World Conference on Photovoltaic Energy Conference (WCPEC-3, May 11-18, 2003, Osaka, Japan). Accepted for publication in WCPEC-3 Proceedings.
- [28] J. Kois, S. Bereznev, E. Mellikov, and A. Öpik, Proceedings of the Estonian Academy of Sciences, Chemistry, Vol. 52 No. 2 June 2003, p. 51–58.
- [29] S. Bereznev, I. Konovalov, A. Öpik, J. Kois and E. Mellikov, submitted to Advanced Functional Materials.
- [30] S. Bereznev, I. Konovalov, J. Kois, E. Mellikov, A. Öpik, 2003 MRS Spring Meeting, April 21-25, 2003, San Francisco, CA, MRS Symposium Proceedings, Vol. 771 © 2003 Materials Research Society L7.17 (on-line proceedings): [http://www.mrs.org/cgi-bin/check\\_membership\\_access/proceedings/spring2003//L7\\_17.pdf](http://www.mrs.org/cgi-bin/check_membership_access/proceedings/spring2003//L7_17.pdf).
- [31] T. Haalboom, T. Gödecke, F. Ernst, M. Rühle, R. Herberholz, H. W. Schock, Beilharz, K. W. Benz, Inst. of Phys. Conf. Series No 152 (1998) 249.
- [32] M. Altosaar, E. Mellikov, Jap. J. Appl. Phys. 39. (2000) Suppl. 39-1, 65.
- [33] D. Meissner, E. Mellikov, M. Altosaar, Einkristallpulver- und Monokorn-membranherstellung, Patent of Germany #19828310, 6. 09. 2000
- [34] E. Mellikov, M. Altosaar, T. Varema, M. Deppe, C. Wirts, J. Deppe, R. Hiesgen, D. Meissner, Proceedings of 25th IEEE Photovoltaic Specialists Conference, Washington, 1996. p. 877.
- [35] M. Altosaar, A. Jagomägi, M. Kauk, M. Krunks, J. Krustok, E. Mellikov, J. Raudoja, T. Varema, TSF 431-432(2003) 466-469.